Study on the Deformation Law of Foundation Pit with Shared Ground Connecting Walls

Zhongying Xu[1,2], Xin Shao[3], Jianming He[2], Yintao Chen[4] and Lifeng Wang[1,*]

[1] School of Civil Engineering, Zhejiang University of Science & Technology, Hangzhou, 310023, China

[2] Engineering Department, Zhejiang Guang Tian Component Group Co., Hangzhou, 310000, China

[3] Bridge and Tunnel Department, Zhejiang Scientific Research Institute of Transport, Hangzhou, 310005, China

[4] Engineering Management Department, Keqiao District Construction Group Co., Shaoxing, 312030, China

Revista Internacional
Métodos numéricos
para cálculo y diseño en ingeniería
RIMNI
UNIVERSITAT POLITÈCNICA DE CATALUNYA BARCELONATECH
In cooperation with CIMNE

INFORMATION

Keywords:
Adjacent pit excavation
ground connecting wall
surface settlement
horizontal displacement
finite element modeling

DOI: 10.23967/j.rimni.2025.10.56531

SCIPEDIA Revista Internacional de Métodos Numéricos para Cálculo y Diseño en Ingeniería

Revista Internacional Métodos numéricos para cálculo y diseño en ingeniería RIMNI CIMNE

Study on the Deformation Law of Foundation Pit with Shared Ground Connecting Walls

Zhongying Xu[1,2], Xin Shao[3], Jianming He[2], Yintao Chen[4] and Lifeng Wang[1,*]

[1]School of Civil Engineering, Zhejiang University of Science & Technology, Hangzhou, 310023, China

[2]Engineering Department, Zhejiang Guang Tian Component Group Co., Hangzhou, 310000, China

[3]Bridge and Tunnel Department, Zhejiang Scientific Research Institute of Transport, Hangzhou, 310005, China

[4]Engineering Management Department, Keqiao District Construction Group Co., Shaoxing, 312030, China

ABSTRACT

This study comprehensively investigates the mechanical behavior and deformation patterns of adjacent foundation pits sharing a common ground connecting wall. Utilizing a combination of detailed field measurements and finite element modeling, the study simulates the excavation process to analyze the mutual interactions between two adjacent pits of equal depth. Results indicate that the excavation of a subsequent pit influences both surface settlement and the horizontal displacement of the retaining structure of the first-excavated pit. Specifically, the surface settlement outside the first-excavated pit increased by 0.08% H_0 (where H_0 is the excavation depth of the second pit), with the most significant impact occurring at approximately 1.8 H (where H is the excavation depth of the first pit) within the influence range of 0 to 2.9 H from the shared ground connecting wall. Similarly, within the range of 2.76 H, the horizontal displacement of the retaining structure of the first-excavated pit showed the greatest increase at 2 H, reaching 0.086% H_0. Mitigative measures, such as increasing the wall thickness or optimizing the excavation sequence, are found to effectively control deformation. These findings provide valuable insights into the design and construction of excavations involving shared ground connecting walls.

OPEN ACCESS

Received: 24/07/2024

Accepted: 01/11/2024

DOI
10.23967/j.rimni.2025.10.56531

Keywords:
Adjacent pit excavation
ground connecting wall
surface settlement
horizontal displacement
finite element modeling

1 Introduction

The excavation of adjacent pits can significantly impact one another, particularly affecting the later-excavated pit. If not properly managed, this interaction may cause excessive displacement of the pit's enclosure structure or excessive settlement of the surrounding ground surface. Thus, understanding the influence patterns and proposing effective mitigation strategies is essential.

Currently, scholars both domestically and internationally have accumulated a substantial amount of research on the characteristics of enclosure structures during the excavation of single foundation pits. Yang et al. [1] discovered that the enclosure structure experiences its maximum lateral

*Correspondence: Lifeng Wang (wanglfzust@163.com).

displacement near the excavation surface, with the maximum horizontal displacement measuring approximately 0.59% of H (where H represents the excavation depth of the foundation pit). Xu et al. [2] analysed 93 foundation pits in the Shanghai area that used ground walls as enclosure structures. They found that the maximum lateral displacement of the ground wall ranged from 0.1% H to 1.0% H, with an average of 0.42% H. The maximum lateral displacement of the enclosure structure was typically located within the range of $(H - 5)$ to $(H + 5)$. Xu et al. [3] analysed the foundation pit using ground walls and internal support in the geology of Nanjing clay, silt loam, and muddy siltstone. The study concluded that the maximum horizontal displacement of the enclosure structure was between 0.09% H and 0.24% H, with a mean value of 0.13% H. Regarding surface settlement, Clough et al. [4] conducted a worldwide study on surface settlement in hard clay, residual soil, sandy soil, and hard soil pits. They established a correlation between the maximum surface settlement and the excavation depth H. The average value of the maximum surface settlement is approximately 0.15% H. For sandy soil and soft to moderately hard clay, the settlement area range is 2 H, while for hard clay, the settlement area range is 3 H. According to Wang et al. [5], the depth of excavation and the thickness of the soft soil layer behind the wall affect the surface settlement. The maximum value observed through monitoring data ranged from 0.1% to 0.8% H. According to Yu et al. [6], the range of surface settlement around the pit gradually increases with the depth of excavation. The maximum value of surface settlement occurs at a horizontal distance of 0.72 H from the enclosing structure, with a size of about 0.225% H. Woo et al. [7] analysed observation data of pit settlement in the Taiwan Basin and found that excavation caused settlement to occur in a range of (4∼5) H on the ground surface.

The excavation of multiple pits can have complex effects on adjacent pits. Zheng et al. [8] noted that the force situation of an adjacent pit's enclosure structure is more complex than that of independent pits. Tao et al. [9] conducted a numerical simulation study comparing two adjacent foundation pits with large differences in depth and area. They determined the optimal excavation method for controlling the deformation of the enclosure structure, surface settlement, and other characteristics. Tao et al. [10], in their analysis of excavating adjacent pits, found that the proximal enclosure experiences significantly greater displacement than the distal enclosure during synchronous construction. Similarly, Wang et al. [11] concluded that a spacing of less than 2 H between adjacent pits significantly impacts the deformation of the pit enclosure structure, while a spacing greater than 2.5 H has a negligible impact. Gu et al. [12] suggested that using pit block excavation can fully utilize the 'spatial and temporal effects' of pit excavation, reducing construction difficulties, controlling the deformation of the foundation pit, and minimizing surface settlement. Chen [13] observed that when the pit spacing is small, excavation of neighboring pits reduces the displacement of the enclosure structure on the adjacent side of the completed pit, while increasing the displacement on the non-adjacent side. However, when the pit spacing is greater than twice the excavation depth, it has less effect on the surface settlement and horizontal displacement of the enclosure structure. The settlement of soil on the surface between pits gradually disappears when the pit spacing exceeds 50 m. Shen [14] analyzed the interaction of soil bodies among 12 groups of pits that are either independent or share a shared ground connecting wall. The results indicate that excavation of pit groups significantly affects the internal force, deformation, and surrounding environment of the pit. Therefore, strengthening the enclosure structure at the corresponding location is necessary during the excavation of pit groups. Tan et al. [15] analyzed the deformation characteristics of the enclosure structure during the excavation of the pit under the shared wall, using the example of a large volume pit in Shanghai that was divided into two pits by setting up a circular ground wall. They concluded that cylindrical pit excavation has a smaller deformation amplitude and stronger deformation resistance than conventional basement excavation.

In summary, extensive research has been conducted on the interaction between adjacent pit excavations. However, due to the distinct regional characteristics of foundation pit engineering, and the varying soil conditions and support structures in different areas, the displacement of pit enclosure structures and surface settlement can differ significantly. The interaction laws of adjacent pits sharing ground walls, in particular, require further investigation. This paper utilizes on-site measurements to conduct finite element simulations of two adjacent pits with the same depth, connected by a shared ground wall. The goal is to analyze the development patterns of horizontal displacement in the enclosure structure and surface settlement outside the pits, as well as to define the scope of mutual influence caused by the shared ground wall. Based on these findings, corresponding improvement measures are proposed to mitigate the impact within the identified scope of influence. These results provide valuable insights for the design and construction of similar projects.

2 Project Overview

Construction of a group of excavation pits at the site covers an area of 11,716 m^2, with an underground building area of 29,292 m^2. Pits one and two were excavated first, each with a depth of 15.2 m. They share a common ground connecting wall, and the protective structure adopts an underground continuous wall with three supports.The underground continuous wall has a thickness of 800 mm and reaches a depth of 32 m. The supports are arranged at the same height, with the layout shown in Fig. 1. The typical cross-section of the protective structure is shown in Fig. 2. The soil layers from top to bottom mainly include fill soil, clay, silty clay, silty clay with silt, clay, silty sand, rounded gravel, and completely weathered rock.

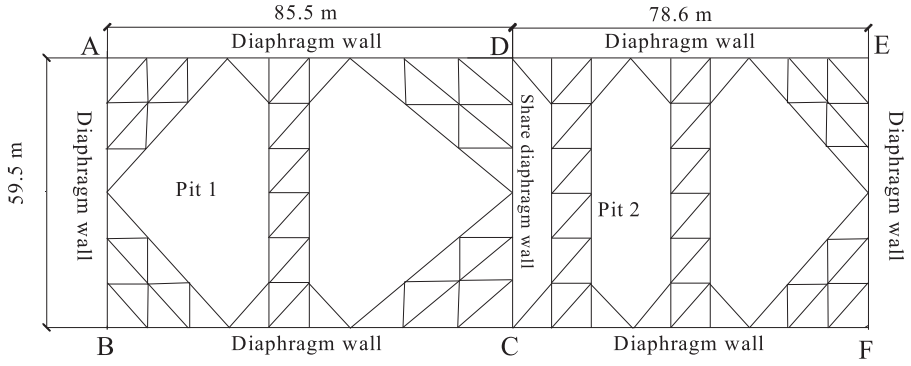

Figure 1: Schematic diagram of pit plan location

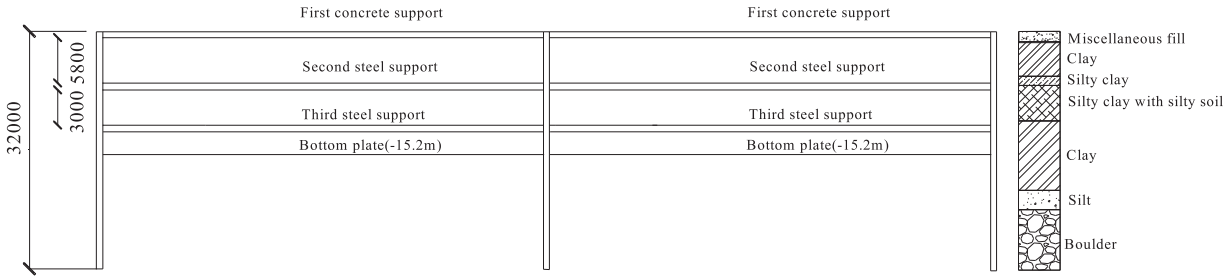

Figure 2: Section of enclosure structure

3 Theoretical Foundations

The project's enclosure structure comprises a ground-connected wall and internal support. According to extensive literature and experience [16], the surface settlement curve outside the pit can be assumed to be notch-shaped, dividing the surface settlement into a triangular and normal distribution curve (see Fig. 3). The inflection point under the normal distribution of the settlement trough is at a distance from the edge of the pit. Please refer to figure for further details.

$$X_0 = H_g \tan 45^\circ - \frac{\varphi}{2}, \tag{1}$$

where X_0 represents the horizontal distance from the edge of the pit to a specific point of interest (in meters), usually related to the geometry of the pit or the extent of settlement influence, H_g represents the depth of the pit (in meters), i.e., the vertical distance from the ground surface to the bottom of the excavation, and φ represents the internal friction angle of the soil (in degrees), which describes the shear strength of the soil.

$$S_{w1} = 2.5\left(\frac{1}{4}X_0\right)\cdot\delta_{m1}, \tag{2}$$

where S_{w1} represents the settlement value associated with the deformation of the pit (in meters), typically indicating the maximum settlement at a specific point, δ_{m1} represents the settlement at a reference point (in meters), usually denoting the observed settlement at a monitoring point during the excavation.

$$\delta_{\mathrm{m1}} = \frac{4S_{w1}}{2.5X_0}, \tag{3}$$

where δ_{m1} represents the settlement at the reference point (in meters) as defined earlier, s_{w1} and x_0 are the same as defined in the previous equations.

$$\Delta\delta = \frac{1}{2}\left(\Delta\delta_{w1} + \Delta\delta_{w2}\right), \tag{4}$$

where $\Delta\delta w_1$ represents the horizontal displacement of the top of the enclosing pile and $\Delta\delta w_2$ represents the horizontal displacement of the bottom of the enclosing pile. Additionally,

$$S_{w2} = \frac{1}{2}X_0\Delta\delta, \tag{5}$$

$$S_{w1} = S_w - S_{w2} = S_w - \frac{1}{2}X_0\Delta\delta, \tag{6}$$

$$\delta_{m1} = \frac{4S_{w1}}{2.5x_0} = \frac{4}{2.5}\left(\frac{S_w - \frac{X_0}{2}\Delta\delta}{X_0}\right) = \frac{4S_w}{2.5X_0} - \frac{2\Delta\delta}{2.5} = \frac{1.6S_w}{X_0} - 0.8\Delta\delta. \tag{7}$$

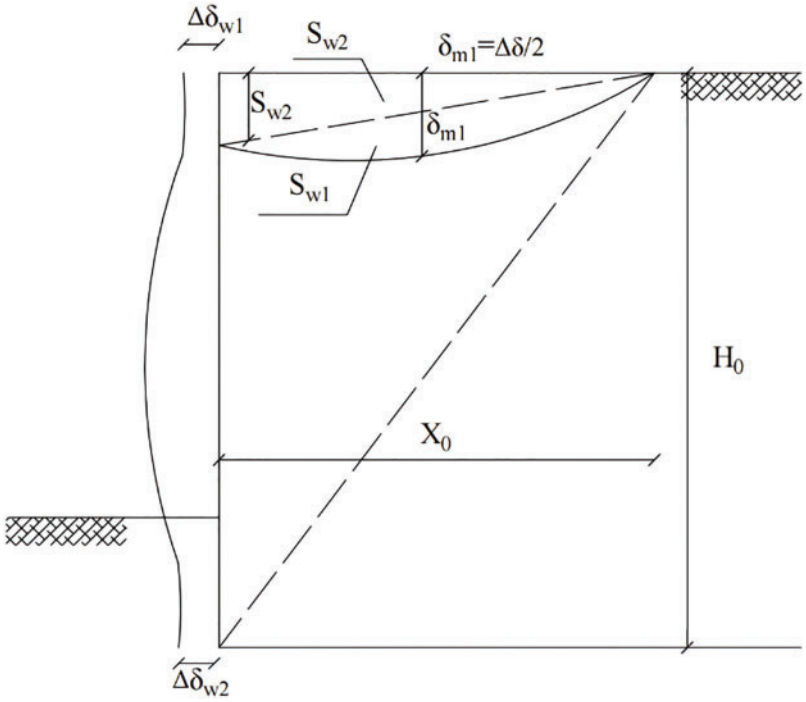

Figure 3: Calculation model of exponential settlement curve

Then the displacement of each settlement point is:

$$\Delta\delta_i = \delta_{m1}\left(\frac{x_i}{x_0}\right)^2. \tag{8}$$

When $x_i = \frac{1}{2}x_0$, the maximum settlement value typically occurs due to the distribution of settlement effects. In general, settlement impacts follow a certain distribution pattern, which may be symmetrical or gradually decrease over a certain range. The maximum settlement often occurs at the midpoint between the excavation or supporting structure, i.e., at the center of the settlement basin. Physically, at $x_i = \frac{1}{2}x_0$, this corresponds to being at the midpoint or central region of the settlement influence zone, where the deformation or settlement of the soil reaches its peak. This is due to the stress concentration from both sides of the soil, leading to the maximum settlement accumulation at this point. Mathematically, when substituting $x_i = \frac{1}{2}x_0$ into the relevant settlement equation, the result typically shows that the settlement at this location is the largest because the effects from both sides are equal, causing the settlement to amplify. Therefore, at $x_i = \frac{1}{2}x_0$, both physically and mathematically, it can be explained that the maximum settlement occurs at this location. So the maximum settlement value was:

$$\delta_{max} = \delta_{m1} + \delta_{m2} = \delta_{m1} + \frac{\Delta\delta}{2} = \frac{1.6S_w}{x_0} - 0.3\Delta\delta. \tag{9}$$

Based on the formula provided, the maximum surface settlement value is 18.2 mm, slightly larger than the monitored value of 18.4 mm shown in Fig. 4. The measured and theoretical values of surface settlement are in good agreement, with the measured values being larger than the theoretical values overall. This is due to the compression and settling of the soil layer during the excavation process.

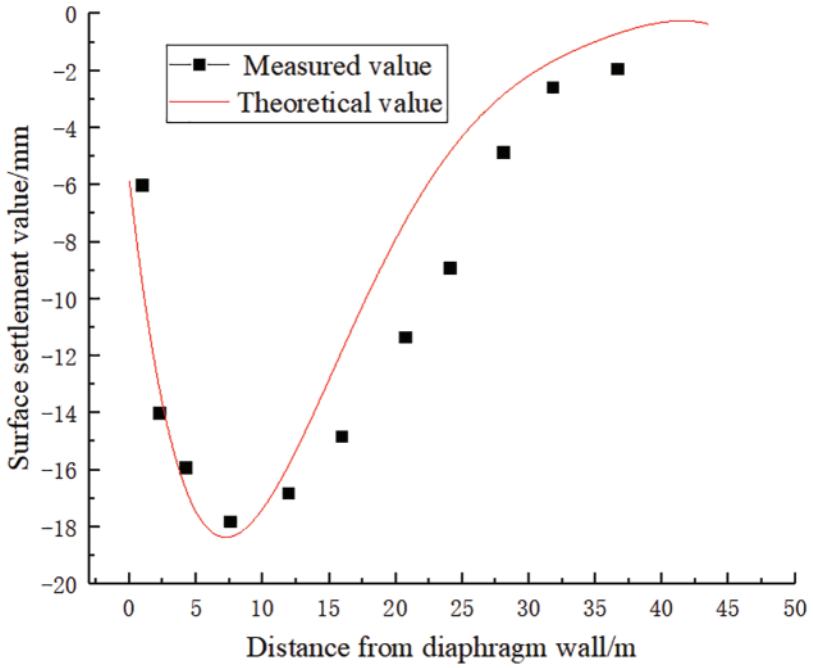

Figure 4: Comparison of measured and theoretical values of surface settlement

4 Numerical Simulation Analysis

4.1 Model Building

The model dimensions are 500 m × 400 m × 60 m. To eliminate any influence from the model boundary, a distance of 100 m is maintained between the boundary and the pit enclosure structure, exceeding the specification requirement of 3 H. The construction simulation follows the actual construction sequence, as detailed in Table 1.

Table 1: Construction simulation conditions serial

Step number	Working condition	Step number	Working condition
1	Initial geostress balance	9	Excavation of Pit II
2	Excavation of Pit I	10	Installation of the first concrete support
3	Installation of the first concrete support	11	Excavation of Pit II to a depth of 5.8 m
4	Excavation of Pit I to a depth of 5.8 m	12	Installation of the second steel support
5	Installation of the second steel support	13	Excavation of Pit II to a depth of 10.5 m
6	Excavation of Pit I to a depth of 10.5 m	14	Installation of the third steel support
7	Installation of the third steel support	15	Excavation of Pit II to a depth of 15.2 m
8	Excavation of Pit I to a depth of 15.2 m	16	Installation of the bottom slab in Pit I
		17	Installation of the bottom slab in Pit II

The Hardening Soil Model with Small Strain Stiffness model (HS-Small model) not only accounts for the shear hardening and compression hardening of soil but also accurately captures the reduction

in shear modulus with increasing strain within a small strain range. Consequently, the HS-Small model is adopted as the soil constitutive model in this study. The model parameters were determined through geotechnical tests conducted on soil samples taken directly from the site, ensuring that the parameters align closely with the actual conditions of the soil layers present. These parameters were further validated against relevant literature [17–19] to maintain consistency with established standards. Additionally, the shared ground connecting wall are modeled using the plate element in PLAXIS 3D Finite Element Code for Soil and Rock Analyses., the concrete supports are represented using the beam element, the lattice columns are simulated using the embedded pile element, and the steel supports are modeled with the anchor element. The mechanical parameters for each soil layer are presented in Table 2, while the mechanical parameters of the foundation pit support structure are detailed in Table 3.

Table 2: Mechanical parameters of each soil layer

Serial	Soil layer	$\gamma/(\mathrm{kN\,m^{-3}})$	E_{50}^{ref}/MPA	E_{oed}^{ref}/MPa	E_{ur}^{ref}/MPa	c/kPa	φ	G_0^{ref}	Layer thickness/m
①	Heterogeneous fill	15.5	12	10	36	8	20	36	2.5
②	Clay	18.74	4.8	4	20	9.3	26.1	30	3.02
③	Clay	18.45	7.2	6	30	8	20	40	3.48
④	Silty clay	19.39	8	7	35	8.5	30	45	1.72
⑤	Silty clay with sand	18.98	8	8	40	8	30	50	4.78
⑥	Clay	19.47	8	8	40	9	26	45	9.35
⑦	Silt sand	19.98	12	12	48	5.3	21	180	2.6
⑧	Round gravel	21	15	15	45	0	37	250	8
⑨	Highly weathered siltstone	22	50	50	150	7	30	300	38

Table 3: Mechanical parameters of pit support structure

Title	Serious	Modulus of elasticity	Poisson's ratio	Sizes
The common wall	25 kN m^{-3}	12 MPa	0.3	0.8
The concrete support	21 kN m^{-3}	15 MPa	0.2	$0.9 * 0.9$
The steel support	22 kN m^{-3}	200 GPa	0.3	/

4.2 Model Validation

To ensure the mechanical parameters of the soil and pit support structure in the model are reasonable, we have compared the calculated values of the numerical simulation of the surface settlement and horizontal soil displacement with the measured values. Fig. 5 shows the plan layout of the monitoring points.

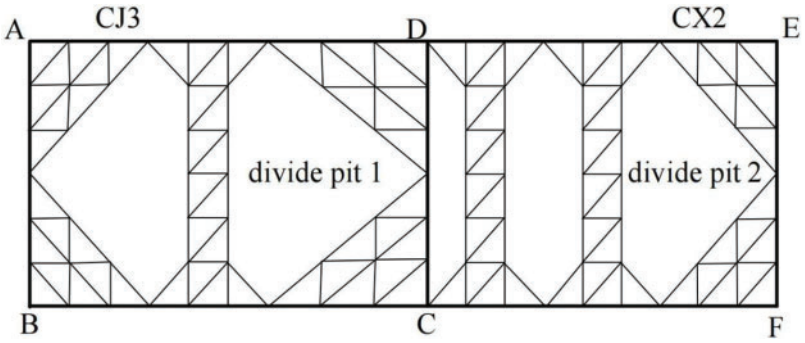

Figure 5: Layout of monitoring points

For the purpose of verifying the accuracy of numerical simulation data, the surface settlement monitoring point CJ3 (monitoring points, see Fig. 5) in the actual project is suitable as it is not surrounded by lorry crushing or heavy stacking. CJ3 is located 15 m away from the AB (Left boundary of the pit, see Fig. 5) enclosure. Fig. 6 shows the comparison between the simulated and measured values at this point. The figure illustrates that the surface settlement at this monitoring point increases continuously with the excavation of the foundation pit. The maximum simulated surface settlement value is −8.14 mm, which closely matches the measured value. The measured value fluctuates during excavation, as the numerical simulation does not consider the influence of load accumulation at the construction site. However, the overall trend of the simulated and measured values is similar, indicating reasonable selection of model parameters.

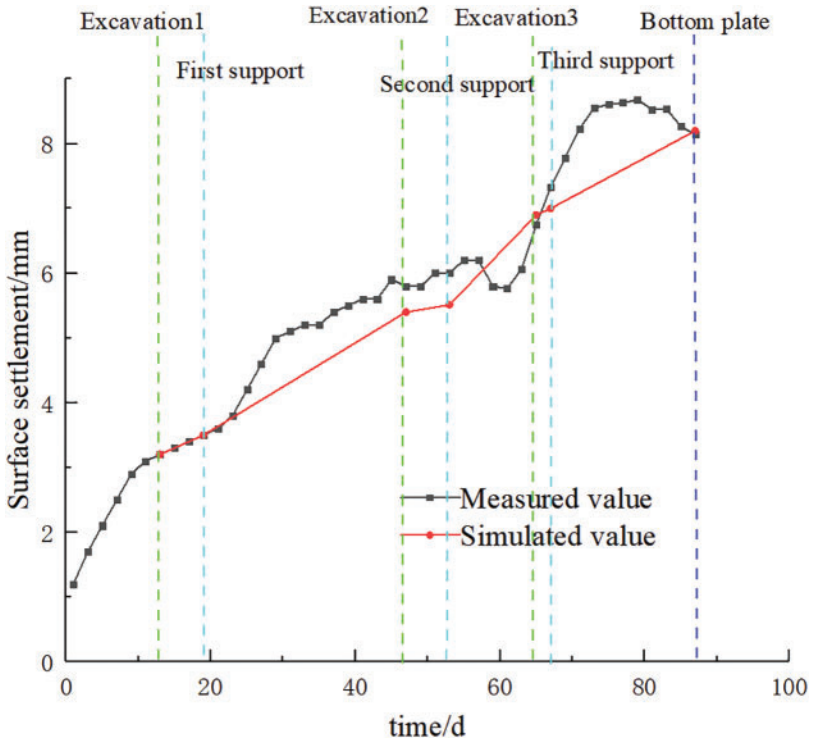

Figure 6: A comparison between the measured and modelled values of surface settlement

Monitoring point CX2 (monitoring points, see Fig. 5) is located 15 m away from the edge of the EF (Right boundary of the pit, see Fig. 5) and is the farthest point from Pit I on Pit II. It is least affected by the excavation of pit 1 and is less susceptible to external factors. This makes it suitable for verifying the accuracy of numerical simulations. The comparison between the measured value and the value shown in Fig. 7 confirms this suitability. The figure shows that the maximum horizontal displacement of the deep soil is 9.3 mm, with the highest value occurring at a depth of 2 m and gradually decreasing thereafter. The maximum simulated horizontal displacement of the deep soil is 9.7 mm, occurring at a depth of 5.7 m, and also decreasing gradually with depth. The numerical values are consistent with the measured values, indicating that the model parameters were selected reasonably.

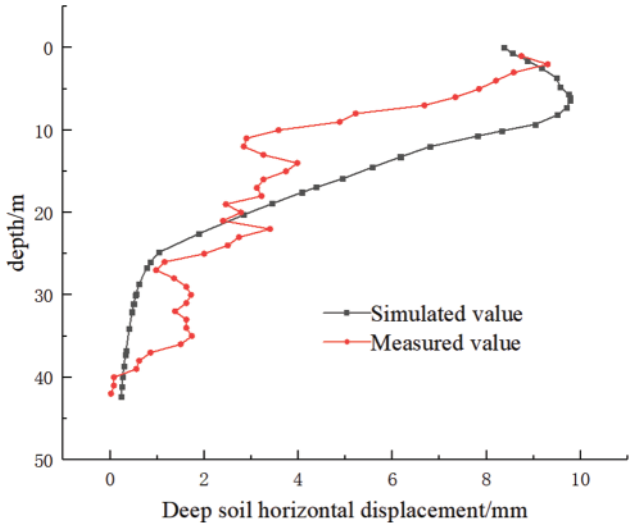

Figure 7: Comparison of horizontal displacements of deep soils

4.3 Simulation and Analysis of Numerical Results

4.3.1 Changing Law of Surface Settlement at the Edge of the Pit

Fig. 8 shows the cloud diagram of surface settlement as Pit I and Pit II were successively excavated to the bottom of the pit. From Fig. 8a, it can be seen that when the excavation of sub-Pit I alone was completed, the settlement of each side of the pit was similar, with the maximum value located in the center of the pit, while the settlement of the corner was the smallest, with a maximum value of 18.4 mm when the excavation was completed to the bottom. From Fig. 8b, it can be seen that when the excavation of Pit II was completed after the excavation of Pit I, the maximum value of surface settlement was 29.7 mm, which was located in the middle of the AD side and moved towards the shared ground connecting wall. After the completion of the excavation of Pit I, the surface settlement on the AB side (distal end) is basically the same as after the excavation of Pit II to the bottom, but the excavation of Pit II has a greater impact on the surface settlement near the shared ground connecting wall. Meanwhile, at some distance from the shared ground connecting walll, the surface settlement is basically unaffected by Pit II.

Fig. 9 illustrates the variation in maximum surface settlement along the AE side outside the pit under different working conditions. Curve I depicts the maximum surface settlement variation following the completion of Pit I's excavation. The settlement is smallest at the pit corners, while the maximum settlement occurs in the middle of the AE side, with a peak located 33 m from the shared

ground connecting wall. Curves II, III, and IV illustrate the variation in maximum surface settlement along the AE side when Pit II is excavated to depths of 5.8, 10.5, and 15.2 m, respectively. At point G, positioned 43.7 m (*2.9 H*) from the shared ground connecting wall on the CD side, the maximum surface settlement remains nearly unchanged from the far side (AB) to point G. However, from point G to the CD side, the settlement gradually increases.

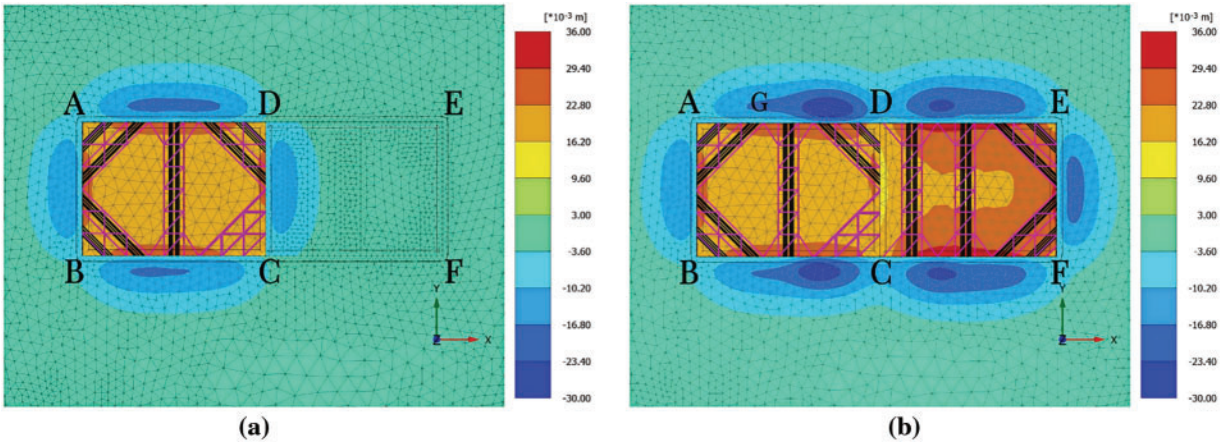

Figure 8: Surface settlement nephogram of Pits I and II excavated to the bottom of the pit, they should be listed as: (a) Separate excavation for Pit I; (b) Pit II excavation

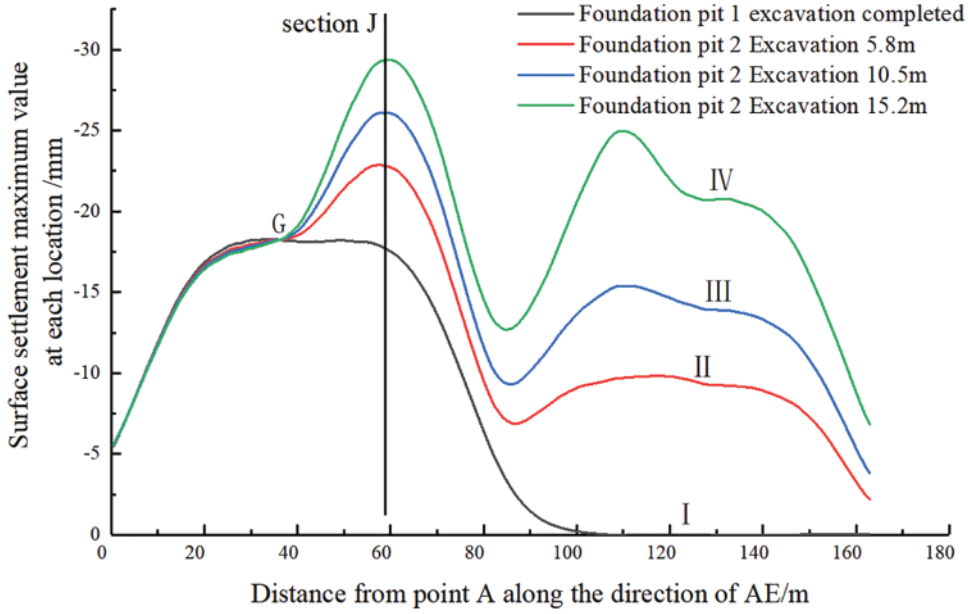

Figure 9: Surface settlement map of the AE edge

Fig. 10 illustrates the relationship between the excavation depth of Pit II and the corresponding change in surface settlement of Pit I. The maximum surface settlements were recorded when Pit II was excavated to depths of 5.8, 10.5, and 15.2 m, resulting in settlements of 23, 26.2, and 29.7 mm, respectively—an increase from the 18.4 mm observed when Pit I was excavated to its full depth alone.

The impact of the continuous excavation of Pit II on the maximum surface settlement of pit I is evident, with contributions ranging from 0.074% H_0 to 0.08% H_0 of Pit II's current excavation depth. Although surface settlement outside the pit continues to increase from section J (1.8 H from side CD) to side CD, the rate of increase gradually diminishes. Simultaneously, the maximum surface settlement along DE, the long side of Pit II, shifts towards the shared ground connecting wall due to the presence of Pit I. The excavation of Pit II affected Pit I within a range of approximately 2.9 H from the shared wall along the AD side. The most significant increase in surface settlement, approximately 0.08% H_0, occurred at 1.8 H from the shared ground connecting wall. In one of the sub-pits, the maximum surface settlement increased by 62%, from 18.4 to 29.7 mm.

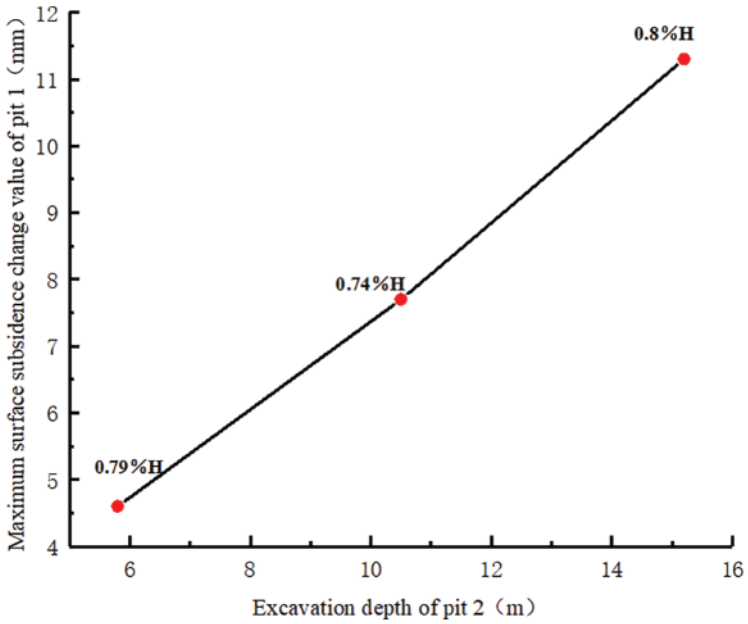

Figure 10: Plot of the ratio of the depth of excavation in Pit II to the change in surface settlement in Pit I

4.3.2 Rule of Horizontal Displacement of Enclosure Structure

Fig. 11 illustrates the horizontal displacement contour plots of the retaining structures for Pit I and Pit II at their final excavation depths. As illustrated in Fig. 11a, upon the completion of Pit I, the horizontal displacement of the retaining structure gradually increases with increasing excavation depth, with the maximum displacement occurring in the lower middle section of the long side, directed inward towards the pit, and reaching 26 mm. Fig. 11b shows that when Pit II is excavated to its full depth, the maximum horizontal displacement of the retaining structure in Pit I increases to 39 mm, a 50% increase compared to the maximum displacement observed after Pit I's excavation. Fig. 11c and d indicates that the maximum displacement of the retaining structure at the far side (AB) remains at 23 mm both before and after the excavation of sub-Pit II, suggesting that the excavation of Pit II has minimal impact on the horizontal displacement of the retaining structure on the far side of Pit I.

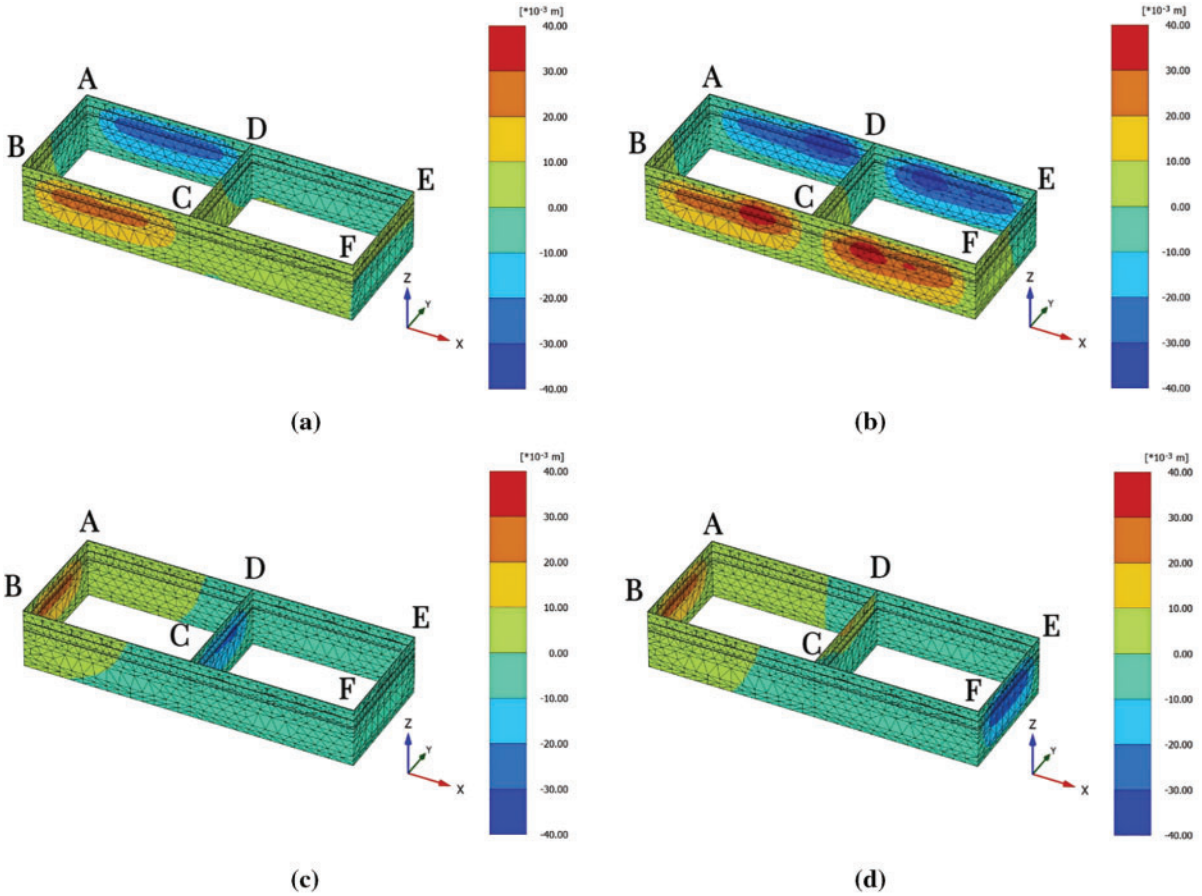

Figure 11: Horizontal displacement of the enclosure structure from the excavation of Pits I and II, they should be listed as: (a) ADE, BCF nephogram at the completion of Pit I excavation; (b) ADE, BCF nephogram at the completion of Pit II excavation; (c) AB, CD, EF nephogram at the completion of Pit I excavation; (d) AB, CD, EF nephogram at the completion of Pit II excavation

Fig. 12 illustrates the variation curve of the maximum horizontal displacement of the enclosure structure along the long side AE of the two pits after the excavation of Pit I and the start of the excavation of Pit II. During the excavation of Pit II, the maximum horizontal displacement shifted from the middle of Pit I towards Pit II, reaching its peak at point J, which is located 31.5 m (2 H) from the shared ground connecting wall. Between points A and G (with point G being 42 m or 2.76 H from the shared ground connecting wall), the subsequent excavation of Pit II had no significant effect on the horizontal displacement of the previously excavated Pit I's enclosure. However, the horizontal displacement gradually increased from point G to section J, reaching its maximum at section J.

Fig. 13 illustrates that upon completion of the excavation of Pit I, the maximum horizontal displacement of the enclosure structure on the AD side reached 26 mm, located 2.3 H from point D. As illustrated, the maximum horizontal displacement of the enclosure structure of Pit I increased to 30.7, 34.5, and 39 mm when the excavation depth of Pit II was at 5.8, 10.5 m, and the bottom of the pit, respectively. This increase corresponds to a change in the horizontal displacement of the enclosure structure from 0.08% H_0 to 0.086% H_0. It is clear that the excavation of adjacent pits influenced the horizontal displacement of the enclosure structure of the first-excavated pit, with an impact range of 0

to 2.76 H from the shared ground connecting wall. Additionally, the excavation of Pit II led to a 50% increase in the maximum horizontal displacement of Pit I's enclosure, from 0.08% H to 0.086% H_0.

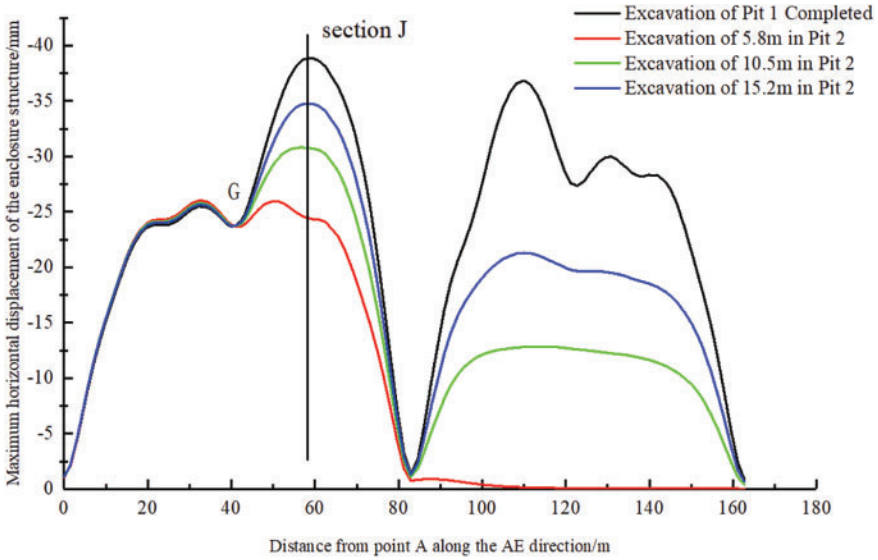

Figure 12: Variation of maximum horizontal displacement of the enclosure at the AE side

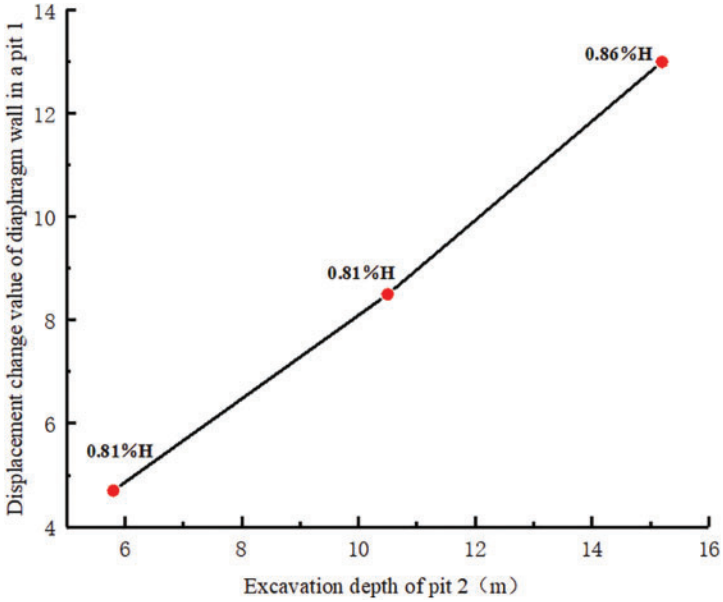

Figure 13: Plot of the ratio of the depth of excavation in Pit II to the change in displacement of the shared ground connecting wall in Pit I

4.3.3 Mechanistic Explanation of Observed Phenomena

The observed phenomenon based on 4.3.1 and 4.3.2, particularly the increased surface settlement and horizontal displacement associated with the excavation of adjacent pits sharing a ground

connecting wall, can be attributed to the complex interaction of soil mechanics and structural responses under excavation-induced stresses.

When two pits are excavated in close proximity, the shared ground connecting wall experiences differential loading from both sides. As one pit is excavated, the lateral earth pressure on the shared wall reduces on the excavation side, while the opposite side remains under higher lateral pressure. This differential loading leads to asymmetrical deformation of the wall, influencing both the wall's horizontal displacement and the surrounding soil's settlement.

The increase in horizontal displacement observed during the excavation of the second pit can be explained by the unloading and reloading effects on the shared wall. Initially, the excavation of the first pit causes the shared wall to displace towards the excavation side due to the reduction in lateral earth pressure. However, as the second pit is excavated, the lateral earth pressure on the opposite side of the wall is reduced, causing a rebound effect that further increases the displacement. This secondary displacement is compounded by the strain-hardening behavior of the soil, where the soil exhibits increased stiffness after initial yielding, leading to a more pronounced displacement response when subjected to further unloading.

Moreover, the observed surface settlement patterns can be mechanistically linked to the redistribution of stresses within the soil mass. As excavation progresses, the reduction in lateral support causes the soil to move towards the excavation, resulting in surface settlement. The shared wall acts as a structural constraint, altering the natural settlement pattern that would be expected if the pits were excavated independently. The presence of the shared wall creates a stress concentration zone where the soil's displacement is maximized, particularly at a distance of approximately 1.8 H from the wall, as identified in the study. This effect is further amplified by the non-linear distribution of soil stiffness, which varies with depth and proximity to the excavation, leading to differential settlement rates across the excavation boundary.

5 Construction Optimisation Analysis

5.1 Use of Row Piles Plus Combination Enclosure

The results indicate that excavating adjacent pits will have a significant impact on the surrounding area of the completed excavation. To mitigate these impacts and ensure the safety of pit excavation, this project proposes unilaterally adding a row of φ600@800 type piles on the outside of the shared ground connecting wall.

The paper uses a row pile support structure, which includes a discounted shared ground connecting wall with internal support and single grouted piles, in its numerical simulation calculations. The row pile support structure is converted to an equivalent thickness of ground wall based on equivalent flexural rigidity. Fig. 14 illustrates the schematic diagram of the pile model equivalent to ground wall, and Eqs. (10) and (11) show the conversion equations.

$$\frac{1}{64}\pi D^4 = \frac{1}{12}(D+t)h^3, \tag{10}$$

$$h = 0.838 \ * \ D \ * \ \sqrt[3]{\frac{1}{1+\frac{t}{D}}}, \tag{11}$$

where D is the diameter of the row of piles, t is the clear distance between the piles, and h is the discounted thickness of the calculated equal stiffness ground wall.

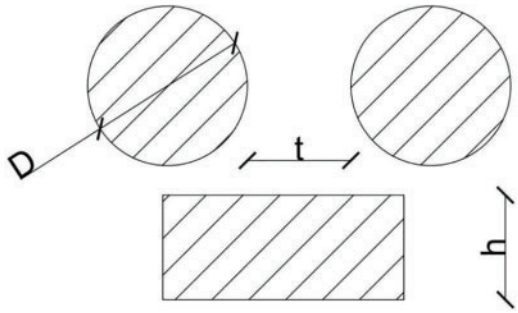

Figure 14: Schematic diagram of row pile equivalent to ground wall model

According to the formula in Eq. (11), the row of piles is equivalent to a ground connecting wall thickness of 0.46 m. As a result, the thickness of the ground connecting wall on the AD side of the model is 1.26 m. The enclosure pit is modelled and analysed with shared ground connecting wall thickness of 0.8 m and an outer wall thickness of 1.26 m on the AD side. Fig. 15 illustrates the comparison of the settlement of the outer surface of the pit with different thicknesses of the shared ground connecting wall. Fig. 15 shows that the maximum surface settlement was 18.4 mm when Pit I was excavated alone to the bottom of the pit using the 0.8 m thickness of shared ground connecting wall as the enclosing structure of the external wall AD. This occurred at about 49.2 m. Excavation of Pit II widened the settlement further to 29.7 mm and shifted the point of maximum surface settlement away from the direction of the pit. Increasing the row of piles reduced the maximum surface settlement outside the pit of this enclosure from 18.4 to 15.2 mm during the excavation of Pit I alone. In addition, the maximum surface settlement in Pit I decreased from 29.7 to 21.8 mm when Pit II was excavated to the bottom of the pit. These results demonstrate that increasing the thickness of the critical cross-section of the enclosure structure effectively reduces deformation in adjacent pits with shared ground connecting wall.

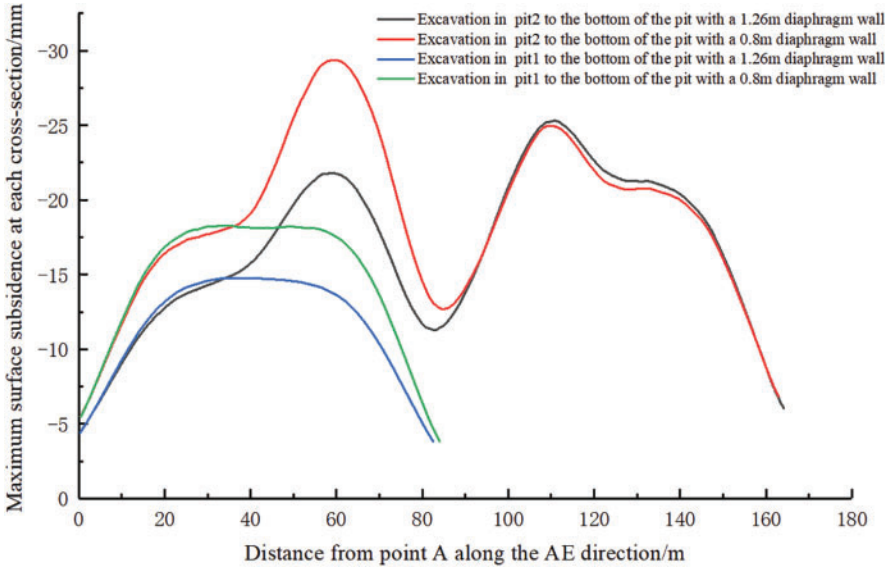

Figure 15: Comparison of the settlement of the outer surface of the pit with different thicknesses of the shared ground connecting wall

5.2 Optimisation of the Construction Sequence

In foundation pit engineering, the foundation pit base plate typically forms a complete support system with the foundation pit support structure. The base plate bears the horizontal and vertical earth pressures of the surrounding soil, supporting the soil and protecting surrounding buildings during excavation of the foundation pit. Therefore, the construction sequence significantly impacts the settlement of the surface at the pit edge, as well as the displacement and deformation of the enclosure structure.

Based on the actual construction conditions, this paper optimises the working conditions as shown in Table 4. The modelling analysis is then carried out based on the two construction sequences, and the calculation results are presented in Fig. 16.

Table 4: Construction sequence schedule

Conditions	Actual construction sequence	Optimisation of construction sequences
1	Construction of the first concrete support in Pit I	Construction of the first concrete support in Pit I
2	Excavation of Pit I to 5.8 m	Excavation of Pit I to 5.8 m
3	Construction of the second steel support	Construction of the second steel support
4	Excavation of Pit I to 10.5 m	Excavation of Pit I to 10.5 m
5	Construction of the third steel support	Construction of the third steel support
6	Excavation of Pit I to 15.2 m	Excavation of Pit I to 15.2 m
7	Construction of the first concrete support in Pit II	Construction of the first concrete support in Pit II
8	Excavation of Pit II to 5.8 m	Construction of the first concrete support in Pit II
9	Construction of the second steel support in Pit II	Excavation of Pit II to 5.8 m
10	Excavation of Pit II to 10.5 m	Construction of the second steel support in Pit II
11	Construction of the third steel support in Pit II	Excavation of Pit II to 10.5 m
12	Excavation of Pit II to 15.2 m	Construction of the third steel support in Pit II
13	Construction of the base slab in Pit I	Excavation of Pit II to 15.2 m
14	Construction of the base slab in Pit II	Construction of the base slab in Pit II

Based on the data presented in Fig. 16, the maximum surface settlement outside the pit is 29.7 mm under the actual construction conditions, occurring at approximately 60 m. Additionally, the maximum horizontal displacement of the enclosure is 39 mm. However, after optimizing the construction conditions, the maximum surface settlement outside the pit is reduced to 21.5 mm, a reduction of 27.6%. Simultaneously, the maximum horizontal displacement of the enclosure structure of the AD ground wall is significantly reduced to 28.7%. By prioritizing the base plate, the structural safety of the excavated pit can be effectively enhanced, and the surface settlement at the edge of the pit can be controlled.

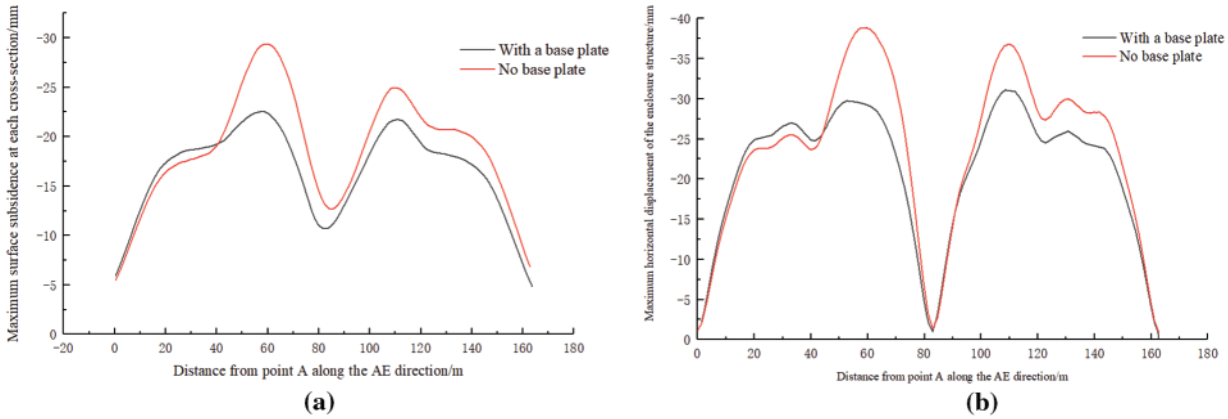

Figure 16: Comparison of surface settlement and horizontal displacement of the enclosure outside the AE side pit, they should be listed as: (a) Comparison of maximum surface settlement values outside the AE side pit; (b) Comparison of maximum horizontal displacement values of the enclosure at the AE side

In comparison to increasing the thickness of the envelope at the hazardous section, setting the footing first in the construction sequence is more effective in controlling the deformation of the footing in the latter excavation pit and reducing the cost. By setting the footing first and excavating the second footing later, better control of the deformation of the footing in the first and later excavation can be achieved.

6 Conclusion

By analysing the different working conditions of the two common shared ground connecting wall adjacent pit footings, this paper investigates the influence of the post-excavation pit on the perimeter structure of the excavated pit and the surface settlement outside the pit, as well as the deformation law of the shared ground connecting wall, and proposes two kinds of construction schemes to reduce the mutual influence of the two footings, and reaches the following conclusions:

(1) During the excavation of adjacent pits shared ground connecting wall, the later-excavated pit significantly influenced the surface settlement of the outer wall of the first-excavated pit, with an impact range of 2.9 H. The maximum surface settlement point was located 1.8 H away from the shared ground connecting wall. Subsequent excavation of pit II increased the surface settlement of the outer wall of the first-excavated pit by between 0.074% H_0 and 0.08% H_0. The excavation of Pit II shifted the point of maximum surface settlement further away from the direction of Pit I.

(2) The excavation of Pit II exerted a more significant influence on the horizontal displacement of the enclosure structure of the Pit I. This impact was most pronounced within a distance of 0 to 2.76 H from the shared ground connecting wall, with the maximum effect observed at 2 H from the shared wall. The increase in maximum horizontal displacement of the enclosure structure due to the excavation of Pit II ranged between 0.08% H_0 and 0.086% H_0.

(3) The use of a combination of row piles and shared ground connecting wall, or thickening the shared ground connecting walls, effectively reduces the impact of the first-excavated pit on the later-excavated pit. When the shared ground connecting wall was thickened by 0.46 m, the maximum

surface settlement outside the pit decreased from 18.4 to 15.2 mm. Additionally, the maximum surface settlement in Pit I decreased from 29.7 to 21.8 mm, with minimal change in the influence range.

(4) Modifying the construction sequence of the project can significantly reduce the mutual influence between adjacent pits of the shared ground connecting wall. Excavating Pit I to the bottom first, then setting the footing before excavating Pit II, is favorable for controlling horizontal displacement of the enclosure structure and surface settlement of both pits. In the absence of special circumstances, it is more appropriate to adopt a construction sequence alteration program.

7 Research Limitations and Future Prospects

This study uses finite element simulations and field measurements to analyze the impact of shared ground connecting wall on horizontal displacement and surface settlement in adjacent excavations. The findings offer important insights for the design and construction of similar projects. However, several limitations should be noted, highlighting areas for future investigation.

7.1 Study Limitations

(1) Site-Specific Conditions: The results are based on specific site conditions, including soil characteristics, retaining structures, and excavation depths. These findings may not be directly applicable to other locations with different geological conditions or construction methods. Future studies should include more diverse sites to assess the generalizability of the conclusions.

(2) Simplified Numerical Models: The study employs the HS-Small constitutive model, which captures nonlinear soil behavior but simplifies complex factors such as soil anisotropy, creep, and groundwater effects. Future research could incorporate more advanced models to better simulate these long-term behaviors.

(3) Limited Construction Sequences: This analysis focuses on two construction sequences, yet variations in sequencing could lead to different outcomes. Future research should explore a wider range of construction strategies, especially under challenging geological conditions.

(4) Boundary Condition Assumptions: The simulations assume ideal boundary conditions, maintaining a distance of 100 m from the excavation to the boundary. This approach overlooks potential interactions with nearby structures. Future work should refine boundary conditions to better reflect real-world scenarios.

(5) Limited Field Data: Although field data were used for model validation, the number and distribution of monitoring points were insufficient to fully capture the complex behavior of the soil and retaining structures. Future studies should incorporate denser monitoring networks to improve accuracy.

(6) Scalability of Results: The study focuses on pits with relatively uniform size and depth. The scalability of these findings to larger or irregularly shaped excavations, or to pits with significantly different dimensions, remains uncertain. Additional research is needed to validate the applicability of the results to more diverse excavation scenarios.

7.2 Future Directions

To address these limitations, future studies could extend the current work in several directions:

(1) Broader Geographical and Site Conditions: Future research should include diverse geological environments and construction methods to validate the general principles of adjacent pit interaction across different regions.

(2) Incorporating More Complex Soil Models: Advanced soil models that account for anisotropy, creep, and dynamic responses in saturated soils should be employed to provide more accurate predictions of soil-structure interactions.

(3) Optimizing Construction Sequences: Future studies should explore a broader array of construction sequences and consider the dynamic loads from construction activities and environmental conditions to identify the most effective methods for reducing deformation and settlement.

(4) Improved Boundary Condition Simulations: Realistic boundary conditions should be introduced in numerical simulations to better capture the interactions between excavations and surrounding infrastructure.

(5) Data-Driven Model Calibration: Machine learning and data-driven methods could be used to enhance model calibration, leveraging extensive field data to improve simulation accuracy and predictive capabilities.

In conclusion, while this study advances our understanding of the interactions between adjacent excavations with shared ground connecting wall, further research is needed to ensure the findings are broadly applicable across different engineering contexts.

Acknowledgement: The authors would like to thank Zhejiang University of Science and Technology, Zhejiang Scientific Research Institute of Transport, Zhejiang Guang Tian Component Group Co., and Keqiao District Construction Group Co. for providing technical support and assistance throughout this research. Special thanks to the engineering teams and researchers who provided field data for model validation, and to all colleagues who offered insightful discussions and feedback during the preparation of this manuscript.

Funding Statement: This research received no external funding.

Author Contributions: Study conception and design: Zhongying Xu, Xin Shao; Data collection: Jianming He, Yintao Chen; Analysis and interpretation of results: Zhongying Xu, Lifeng Wang; Draft manuscript preparation: Lifeng Wang, Jianming He; Manuscript submission and corresponding author responsibilities: Lifeng Wang, Yintao Chen. All authors reviewed the results and approved the final version of the manuscript.

Availability of Data and Materials: This article does not involve data availability and this section is not applicable.

Ethics Approval: Not applicable.

Conflicts of Interest: The authors declare no conflicts of interest to report regarding the present study.

References

1. Yang X, Cao X. Analysis of horizontal displacement deformation of deep excavation support structure. Constr Technol. 2014;43(13):51.
2. Xu Z, Wang J, Wang W. Deformation characteristics of underground continuous walls in deep excavation projects in Shanghai. J Civ Eng. 2008;41(8):81. doi:10.3969/j.issn.1003-312X.2008.08.014.
3. Xu H, Cui W, Hu W. Analysis of deformation characteristics of deep excavation in subway stations in Nanjing area. J Disaster Prev Mitigation Eng. 2018;38(4):599–607.

4. Clough GW, O'Rourke TD. Construction induced movements of *in situ* walls. In: Proceedings of ASCE Conference Design and Performance of Earth Retaining Structures, 1990; New York, NY, USA: Geotechnical Special Publication; p. 439.
5. Wang W, Xu Z, Wang J. Statistical analysis of measured surface deformation characteristics of deep excavation in Shanghai area. Chin J Geotech Eng. 2011;33(11):1659. doi:10.11779/CJGE2011S1110.
6. Yu Q, Wang L, Chen Q. Study on settlement law of buildings around subway station deep foundation pit. Sci Tech Bull. 2020;36(1):105.
7. Woo SM, Moh ZC. Geotechnical characteristics of soils in Taipei Basin. In: Proceedings of 10th Southeast Asian Geotechnical Conference, 1990; Taipei, Taiwan; p. 51–63.
8. Zheng G, Pan J, Cheng X, Bai R, Du Y, Diao Y, et al. Use of grouting to control horizontal tunnel deformation induced by adjacent excavation. J Geotech Geoenviron Eng. 2020;146(7):75. doi:10.1061/(ASCE)GT.1943-5606.0002276.
9. Tao Y, Lv S, Yang P, Zhang T, Wang X. Optimization study on excavation sequence of adjacent deep and shallow foundation pits in Nanjing Jiangbei New Area. J Archit Sci Eng. 2021;38(6):108.
10. Tao D, Zhang H, Kong D. Analysis of mutual influence of adjacent foundation pits excavation in soft soil area. J Water Resour Archit Eng. 2020;18(6):57.
11. Wang W, Si J, Zhang D. Analysis of deformation control during excavation of adjacent foundation pits. China Munic Eng. 2019;206(5):67+109.
12. Gu X, Wang D, Zhang X, Ding Z. Discussion on segmented construction of long and narrow deep foundation pits in complex small underground spaces. Munic Technol. 2017;35(4):181.
13. Chen X. Study on the safety distance of adjacent large deep foundation pits and analysis of cross construction influence," (M.S. Thesis), School of Civil Engineering, Zhejiang University of Technology: Hangzhou, China; 2018.
14. Shen J. Analyses and countermeasures on interaction among large-scale group excavation projects. Chin J Geotech Eng. 2012;34:272. doi:10.3969/j.issn.1000-4548.2012.02.024.
15. Tan Y, Wang D. Characteristics of a large-scale deep foundation pit excavated by the central-island technique in Shanghai soft clay. I: bottom-up construction of the central cylindrical shaft. J Geotech Geoenviron Eng. 2013;139(11):1875–93. doi:10.1061/(ASCE)GT.1943-5606.0000928.
16. Peng T. "Study on deformation of deep excavation retaining structures and surrounding ground settlement in a certain area of rail transit," (M.S. Thesis), Hefei University of Technology: Hefei, China; 2018.
17. Wang W, Wang H, Xu Z. Study on the parameters of HS-Small model of soil in numerical analysis of foundation pit excavation in Shanghai area. Rock Soil Mech. 2013;34(6):1766. doi:10.16285/j.rsm.2013.06.011.
18. Schanz T, Vermeer PA, Bonnier PG. The hardening soil model: formulation and verification. In: Beyond 2000 in Computational Geotechnics; 1999. p. 281–96.
19. Ng CWW. "An evaluation of soil-structure interaction associated with a multi-propped excavation," (Ph.D. Dissertation), University of Bristol: Bristol, UK; 1992.